PHYSICAL REVIEW E **78**, 035302(R) (2008)

Capillary-driven instability of immiscible fluid interfaces flowing in parallel in porous media

Thomas Ramstad* and Alex Hansen†

Department of Physics, Norwegian University of Science and Technology, N-7491 Trondheim, Norway and Numerical Rocks AS, Stiklestadveien 1, N-7041 Trondheim, Norway

(Received 19 September 2007; revised manuscript received 22 August 2008; published 18 September 2008)

When immiscible wetting and nonwetting fluids move in parallel in a porous medium, an instability may occur at sufficiently high capillary numbers so that interfaces between the fluids initially held in place by the porous medium are mobilized. A boundary zone containing bubbles of both fluids evolves, which has a well-defined thickness. This zone moves at constant average speed toward the nonwetting fluid. A diffusive current of bubbles of nonwetting fluid into the wetting fluid is set up.

DOI: 10.1103/PhysRevE.78.035302 PACS number(s): 47.20.Ft, 47.56.+r

When a fluid displaces another one in a porous medium the interface separating the two fluids may become unstable. In the case of two-phase immiscible displacement, local capillary barriers on pore-scale levels affect the behavior on larger scales, and it turns out that there is an extraordinary richness to the ways instabilities occur and how the separating interface subsequently develops. Depending on several flow properties like the viscosity ratio, wetting properties with respect to the porous medium, and how fast the displacement occurs, a wide range of behaviors is found in both drainage and imbibition ranging from pure invasion percolation to viscous fingering [1,2]. A huge effort has gone into classifying and understanding this rich behavior, both from a fundamental scientific point of view, and also due to its importance in a number of very important fields ranging from oil recovery, to spreading of pollutants in the ground water, to problems related to CO_2 sequestering.

It is then surprising to discover that the related problem of immiscible fluids flowing in parallel to the interface between them rather than normal to it in a porous medium has received very little attention in comparison. Such parallel flow is, e.g., seen in connection with fully developed viscous fingers [3] and in connection with flow in stratified reservoirs [4–8]. When the flow rate is low so that capillary forces dominate at the interface, the parallel interface is stable and each phase behaves as in a single-phase flow system. Nevertheless, it has been recognized that above a certain threshold in the flow rate, but where capillary forces still dominate, imbibition processes become important in the evolution of the interface and hence the cross flow of the immiscible fluids. However, at larger flow rates, where viscous forces dominate, shear-driven Kelvin-Helmholtz-type instabilities are believed to occur [9–11]. Both theoretical and experimental work has been invested in studying the Kelvin-Helmholtz instability in vertical Hele-Shaw cells [3,12,13], as it provides a model for parallel flow in porous media in the viscous regime.

It is the aim of this Rapid Communication to investigate the instability that occurs at the interface between two immiscible fluids flowing in parallel in a regime where capillary effects *cannot* be ignored. This regime has remained essentially untouched in the literature. We find that, above a threshold flow rate and with a viscosity ratio between the two fluids favoring the formation of viscous fingers, the interface becomes unstable, and a boundary zone appears containing intermixed bubbles of both fluids. This boundary zone has a well-defined width and moves at constant average speed toward the nonwetting fluid. A diffusive current of bubbles of nonwetting fluid into the wetting fluid is set up, but the situation of bubbles of wetting fluid entering the nonwetting fluid is absent.

This instability may prove to be an important mechanism for mixing nonwetting fluid into wetting fluid. A practical application may be CO_2 sequestering in porous rock formations. A less-wetting gas is blown into a porous medium which is already saturated by a more wetting fluid. A mixing zone will then form at the boundary between the gas and the fluid where gas bubbles will be generated. These bubbles are then transported into the wetting fluid where they eventually are absorbed.

We study this instability here using a two-dimensional network simulator first developed by Aker *et al.* [14] with later extensions by Knudsen *et al.* [15] and Ramstad and Hansen [16]. The network forms a square lattice oriented at 45° with respect to the overall flow direction. Each link forms an hourglass-shaped tube. Disorder is introduced in the model by having the average tube radius r be drawn from a flat distribution on the interval $r \in (0.1\ell, 0.4\ell)$, where ℓ is the link length. Capillary pressure in the links is caused by the presence of interfaces in them.

As the tubes are hourglass shaped, the capillary pressure difference caused by a meniscus at position x, the distance from one of the two nodes it is attached to, is given by $p_c \propto 1-\cos(2\pi x/\ell)$. We assume cylindrical tubes so that the flow rate q in a tube is given by the Hagen-Poiseulle relation from laminar flow

$$q = -\frac{\pi r^4}{8\ell\mu_{\text{eff}}}\left(\Delta p - \sum p_c\right), \tag{1}$$

where Δp is the pressure difference between the nodes connected by the tube. The effective viscosity is the volume-weighted average of the viscosities of the fluids contained in the tube. The sum runs over the number of menisci in the

*thomas@numericalrocks.com
†Alex.Hansen@ntnu.no

tube. We accept up to ten menisci in any given tube. If this number is exceeded or the distance between two bubbles is too small, we merge the mensici.

The flow equations are solved by assuming flux conservation at each node, i.e., invoking the Kirchhoff equations. This is done by defining a pressure p at each node. We use the conjugate gradient method for this [17]. After the node pressures have been determined, the positions of the menisci are integrated forward by an adaptive time step Δt so that no single meniscus movement exceeds one-tenth of a tube length ℓ. When menisci reach the ends of a tube, they are moved into the other eligible tubes connected to that node. For details, see [15].

The flow of the two fluids in the network is controlled by the ratio between capillary and viscous forces at the pore level and quantified through the capillary number

$$\mathrm{Ca} = \frac{\mu Q_{\mathrm{tot}}}{\gamma \Sigma}, \tag{2}$$

where μ is the largest viscosity of the two immiscible fluids, Σ is the cross-sectional area of the network, and Q_{tot} is the total flux through this area.

In addition to the capillary number, the ratio between the viscosities of the two fluids forms the second dimensionless number to control the flow,

$$M = \frac{\mu_{\mathrm{nw}}}{\mu_{\mathrm{w}}}. \tag{3}$$

We set $M=1$ in the following. Hence, there is initially no pronounced shear in the flow patterns in the network.

We implement periodic boundary conditions in the average flow direction [15,16]. This implies that the flow configurations experience no boundaries in the flow direction, and the fluid configurations may develop over large times and distances. There is no periodicity in the direction normal to the average flow direction. The boundaries parallel to the average flow direction are in contact with a reservoir of either wetting or nonwetting fluid. A constant pressure drop ΔP is set up across the network in the average flow direction, causing the total flux Q_{tot}.

The network is prepared either with a band of nonwetting fluid parallel to the average flow direction, surrounded by wetting fluid, or vice versa. Hence, the saturation of nonwetting fluid, S_{nw}, and wetting fluid, S_{w}, is nonuniform. We show in Fig. 1 the network initially prepared with a band of nonwetting fluid in the middle. If the pressure drop ΔP is too small, the interfaces in the tubes forming the boundaries between the two fluid types will be stabilized by the capillary pressures, and the boundaries are stable. However, when the pressure difference is above a minimal value so that the initial capillary number $\mathrm{Ca}_{\mathrm{init}} > \mathrm{Ca}_{\mathrm{min}}$, the boundaries destabilize and the system evolves.

Early in the evolution of the system, fingers of nonwetting fluid form when the viscosity ratio between the two fluids allows this. This is a signature of unstable nonwetting front propagation in the viscous regime. The fingers are bent in the direction of the average flow. Due to the flow typically being at an angle compared to the fingers, they are susceptible to

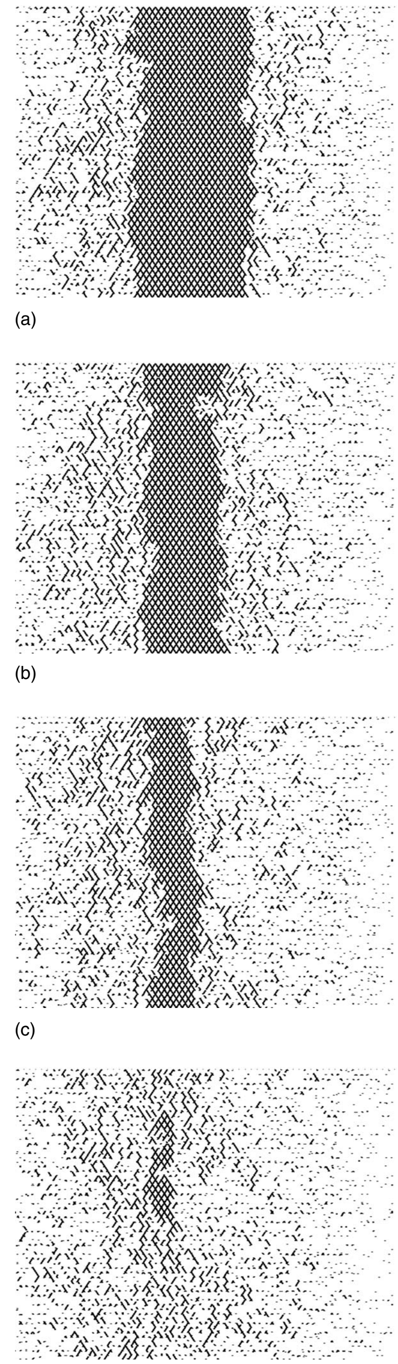

FIG. 1. Different stages of the development of an initially straight band of nonwetting fluid (black) inside a region filled with wetting fluid (white). The flow is from top to bottom with periodic boundary conditions in this direction. The boundaries are open in the transverse direction. The size of the network is $L_x \times L_y = 64 \times 64$.

break up. The broken-off fingers form bubbles that migrate into the wetting fluid, and consequently the wetting fluid also migrates into the nonwetting fluid. This is due to the appearance of an effective pressure gradient $\Delta P_{\perp}$ normal to the average flow direction across the boundary region between the two fluids. This gradient is in turn due to the appearance

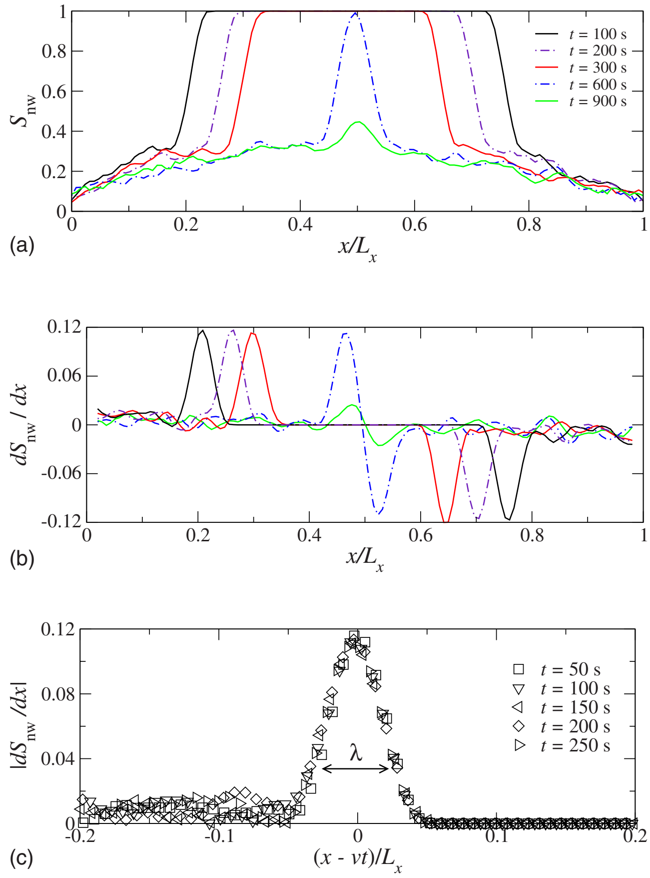

FIG. 2. (Color online) (a) S_{nw} vs x for different average times t, (b) dS_{nw}/dx vs x for different t which correspond to (a), and (c) dS_{nw}/dx vs $(x-vt)/L_x$ for different t for a moving front with starting point $x_0=0$. All figures are for an $L_x \times L_y = 128\times 32$ lattice with open boundaries in the direction parallel to the overall flow and with $\mathrm{Ca}_{\mathrm{init}}=0.03$ and constant pressure drop $\Delta P=3.0$ kPa over the model.

of a gradient in the effective permeability. The effective pressure gradient $\Delta P_{\perp}$ leads to imbibition of the wetting fluid into the nonwetting region. This process creates a compact front and a saturation profile moving in the direction normal to the average flow direction, resembling that of Buckley-Leverett flow [2].

There is a length scale λ associated with the saturation profile. We define it through the width of the bell-shaped nonwetting saturation gradient as shown in Fig. 2 based on an average over five samples. From the motion of the two maxima of dS_{nw}/dx along the x axis, which is the direction normal to the average flow direction, we determine the mean velocity of the nonwetting saturation profile. The data collapse shown in Fig. 2(c), where dS_{nw}/dx is plotted against $(x-vt)/L_x$, shows that the mean velocity v of the profile is constant and the shape of the profile is also constant. The length scale λ is for this system $\lambda/L_x \approx 0.04$. Hence, unlike the Kelvin-Helmholz shear instability, the interfacial instability between two different fluids in a porous medium proceeds through the creation of a well-defined saturation profile characterized by a length scale λ and an average speed v which remains constant.

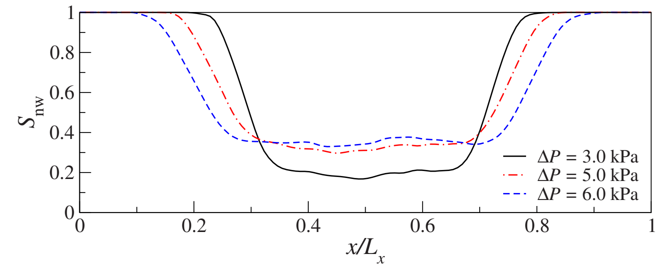

FIG. 3. (Color online) Nonwetting saturation profiles for the initial configuration of a band of wetting fluid surrounded by nonwetting fluid. The profile stabilizes at different levels for different ΔP. For higher ΔP the saturation S_{nw} in the boundary region stabilizes at a higher level and the wetting front advances further.

The shape of the nonwetting saturation profile corresponds to there being a boundary region where bubbles are created. This boundary region moves into the nonwetting zone. There are no bubbles migrating into this zone ahead of the moving boundary region. On the other side, there is a diffusion current of bubbles of nonwetting fluid into the wetting zone. The diffusing bubbles stem from the nonwetting fingers that break off because the average flow is at an angle with respect to the fingers. When the two approaching boundary regions eventually meet, the middle nonwetting band is disconnected as shown in the last picture of the sequence shown in Fig. 1.

We now reverse the initial configuration so that a band of wetting fluid is surrounded by nonwetting fluid. We show in Fig. 3 the evolution of the nonwetting saturation profile as a function of time. As before, boundary regions where bubbles form are created. However, after some initial time, they stabilize and do not move. This is in sharp contrast to the previous situation where the boundary regions move with constant mean velocity. It is caused by there being no bubble transport outside the boundary region and into the nonwetting region. Inside the wetting band, there is diffusive bubble transport, but, as the width of the band is finite and it is surrounded by bubble-generating boundary regions on both sides, the net diffusive current stabilizes at zero.

We consider in the following the evolution of the total flow rate Q_{tot} as the system evolves for both configurations we have studied. We consider first the case of a nonwetting fluid band surrounded by wetting fluid. As the flow is sustained by a constant pressure drop across the network in the average flow direction, ΔP, the total flow rate Q_{tot} will at all times be proportional to the permeability of the network. We show in Fig. 4 the evolution of the total flow rate as a function of time for networks initially prepared with a nonwetting band in the middle and with a wetting band in the middle. We analyze first the case when the network starts with a nonwetting band in the middle. The evolution of Q_{tot} for two different pressure drops is shown in Fig. 4. We see that, for both pressure drops, Q_{tot} decreases linearly in time after an initial transient. In the case of the larger pressure drop, the gray (red online) curve, the flow rate starts increasing again, reaching essentially the flow rate it had initially. This behavior can be understood as follows. After the initial transient and before the rapid increase of Q_{tot} in the high-ΔP case, the

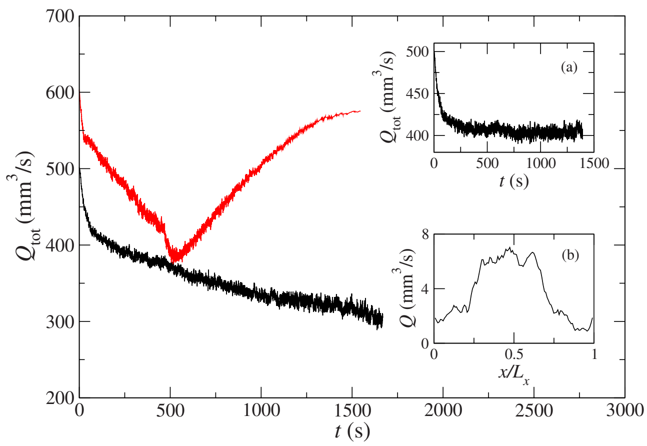

FIG. 4. (Color online) Q_{tot} as a function of time for constant pressure differences $\Delta P=3.0$ (black) and 5.0 kPa [gray (red online)], when the middle band is nonwetting. Inset (a) shows the same for $\Delta P=3.0$ kPa when the middle band is wetting. Inset (b) shows the flux profile normal to the flow profile for an initial nonwetting band in the middle and $\Delta P=3.0$ kPa.

system consists of three zones: (1) a nonwetting zone characterized by an effective local permeability k_{nw}, (2) a boundary zone characterized by a local permeability k_{λ}, and (3) a zone where nonwetting fluid forms diffusing bubbles in the wetting fluid. The local permeability here is k_{mix}. If the width of the nonwetting zone is ℓ_{nw}, that of the boundary zone is λ, and that of the mixed zone is ℓ_{mix}, then the total permeability of the network is given by

$$k_{\mathrm{eff}} = k_{\mathrm{mix}}\frac{2\ell_{\mathrm{mix}}}{L_x} + k_{\lambda}\frac{2\lambda}{L_x} + k_{\mathrm{nw}}\frac{\ell_{\mathrm{nw}}}{L_x}. \tag{4}$$

As the boundary region moves with constant average speed v, we have that $\ell_{\mathrm{mix}}=\ell_{\mathrm{mix},0}+vt$ and since $L_x=2\ell_{\mathrm{mix}}+2\lambda+\ell_{\mathrm{nw}}$, it follows that $\ell_{\mathrm{nw}}=L_x-2\ell_{\mathrm{mix},0}-2\lambda-2vt$. Inserting these two equations in Eq. (4) gives

$$k_{\mathrm{eff}} = k_{\mathrm{eff},0} - \frac{2vt}{L_x}(k_{\mathrm{nw}} - k_{\mathrm{mix}}). \tag{5}$$

Since the viscosities of the two fluids are equal, $Q_{\mathrm{tot}} \propto k_{\mathrm{eff}}$. As k_{nw} is larger than k_{mix}, the total flow rate Q_{tot} falls off with time.

Figure 4 shows that, at a larger pressure difference, the total flow rate starts increasing again after the linear regime we have just described. This is due to the nonwetting band in the middle having been depleted and the nonwetting bubbles diffusing out of the network. Thus the network is being depleted of nonwetting fluid and hence interfaces, which lowers the effective permeability. The opposite situation, a middle wetting band, is shown in inset (a) in Fig. 4. We see that the total flow rate saturates, indicating that the system enters a steady state as already discussed in connection with Fig. 3.

We have in our numerical experiments kept the pressure difference across the network constant. If we rather had kept the total flow rate Q_{tot} constant, the instability that sets in when $\mathrm{Ca} > \mathrm{Ca}_{\mathrm{min}}$ will be much more violent. This is so since the pressure drop ΔP will increase to keep Q_{tot}, leading in turn to an acceleration of the boundary region.

In this Rapid Communication, we have investigated the stability where two different fluids flow parallel to each other. We find that, under constant pressure conditions, for a sufficiently high capillary number a boundary region develops with a well-defined width when the viscosity ratio between the two fluids favors the formation of viscous fingers. This region, which essentially is foam, moves at a constant average speed into the nonwetting region. On the wetting side, a diffusive current of nonwetting bubbles develops away from the boundary zone. It would be of great interest to see this instability reproduced in the laboratory, e.g., in two-dimensional glass-bead-filled Hele-Shaw cells.

We acknowledge very interesting and useful discussions with E. G. Flekkøy, H. A. Knudsen, K. J. Måløy, and P.-E. Øren. This work has been supported by Norwegian Research Council Grant No. 154535/432. A.H. thanks Numerical Rocks AS for their hospitality.

[1] F. A. L. Dullien, *Porous Media: Fluid Transport and Pore Structure*, 2nd ed. (Academic, San Diego, 1992).
[2] M. Sahimi, *Flow and Transport in Porous Media and Fractured Rock* (VCH, Weinheim, 1995). See Chap. 12 for a comprehensive review of instabilities of immiscible displacement.
[3] M. Zeybek and Y. C. Yortsos, J. Fluid Mech. **241**, 421 (1992).
[4] K. R. Coats, J. R. Dempsey, and J. H. Anderson, Soc. Pet. Eng. J. **11**, 63 (1971).
[5] Y. Yokoyama and L. W. Lake, 56th Annual Fall Technical Conference and Exhibition SPE-AIME, Paper No. SPE10109 (1981).
[6] V. J. Zapata and L. W. Lake, 56th Annual Fall Technical Conference and Exhibition SPE-AIME, Paper No. SPE10111 (1981).
[7] F. J. Fayers, SPE Reservoir Eng. **3**, 311 (1988).
[8] F. J. Fayers and T. M. J. Newley, SPE Reservoir Eng. **3**, 542 (1988).
[9] H. H. Bau, Phys. Fluids **25**, 1719 (1982).
[10] M. Panfilov and M. Buès, J. Fluid Mech. **473**, 59 (2002).
[11] G. M. Moatimid and Y. O. El-Dib, Physica A **333**, 41 (2004).
[12] P. Gondret and M. Rabaud, Phys. Fluids **9**, 3267 (1997).
[13] P. Gondret, N. Rakotomalala, M. Rabaud, D. Salin, and P. Watzky, Phys. Fluids **9**, 1841 (1997).
[14] E. Aker, K. J. Måløy, A. Hansen, and G. G. Batrouni, Transp. Porous Media **32**, 163 (1998).
[15] H. A. Knudsen, E. Aker and A. Hansen, Transp. Porous Media **47**, 99 (2002).
[16] T. Ramstad and A. Hansen, Phys. Rev. E **73**, 026306 (2006).
[17] G. G. Batrouni and A. Hansen, J. Stat. Phys. **52**, 747 (1988).